V European Conference on Computational Fluid Dynamics
ECCOMAS CFD 2010
J. C. F. Pereira and A. Sequeira (Eds)
Lisbon, Portugal, 14–17 June 2010

HYDROGEN COMBUSTION IN A DOUBLE CAVITY TRAPPED VORTEX COMBUSTOR

A. Di Marco[*], R. Camussi[†], and S. Giammartini[††]

[*†]University Roma TRE, Industrial and Mechanical Engineering Department
Via della Vasca Navale 74, 00146 Rome Italy
e-mail: (adimarco,camussi)@uniroma3.it

[††]ENEA Casaccia, TER-IMP
Via Anguillarese 301, 00123 S.M. Galeria Rome Italy
e-mail stefano.giammartini@enea.it

Key words: Combustion, Hydrogen, Trapped Vortex.

Abstract. *In the present study numerical simulations are performed to characterize the hydrogen combustion in a double cavity Trapped-Vortex Combustor (TVC). This combustor utilizes two trapped vortices in two cavities to improve flame stability and to provide low pressure drop. Good performances characteristics are obtained injecting a sufficient amount of fuel and air directly into the first cavity. The two cavities are obtained mounting three axisymmetric disks on a tube passing through their centrelines. The geometry and the configuration of this TVC are very similar to that studied by Hsu et al. and refer to a facility in the Casaccia (Rome) research center of the Italian National Agency for New Technologies, Energy and the Environment (ENEA). The numerical studies were made using a commercial 3-D CFD code. A turbulent steady-state model with finite rate chemistry and second-order accuracy is used to simulate the TVC flowfields. The turbulence-chemistry interaction is provided by the Eddy Dissipation Concept (EDC). In the present analysis of reacting flow the chemical kinetic model needed to simulate the hydrogen combustion consists of 37 reactions involving 14 species. In order to evaluate the thermo fluid dynamics in the TVC a parametric study has been conducted. Variable parameters include the length of the first cavity, the power, the equivalence ratio, the humidity of the air and the inlet air composition and temperature ratio, the humidity of the air and the inlet air composition and temperature. The simulations are made with the aim to understand the behaviour of the combustor in different working conditions, to verify eventually transient effects in the cavities and to describe the peculiar flow structures of this kind of combustor. Therefore the analysis presented is focused on describing the essential features of the TVC with particular regard on the temperature, the emissions, the velocity flow fields and the spectra, the last obtained analyzing unsteady data from some probes put in the computational domain. Results from the analysis provide valuable information on the flow and flame structure and on the combustion process demonstrating the versatility and efficiency of burning hydrogen in a double cavity TVC.*

1 INTRODUCTION

Depending on the operating range, important design criteria for combustion devices are the avoidance of flashback and liftoff, two conditions of instability. Flashback occurs when the flame enters and propagates through the burner tube or port without quenching; while liftoff is the condition where the flame is not attached to the burner tube or port hub, rather, is stabilized at some distance from the port. A poor stability of the flame can be obtained attempting to burn fuel in lean mixture combustion regimes to reduce the consumption or the pollutant emissions (furnaces, aircraft engines, turbo-reactors, etc.).

Combustion stability is often achieved through the use of recirculation zones to provide a continuous ignition source which facilitates the mixing of hot combustion products with the incoming fuel and air mixture. Swirl vanes, bluff bodies and rearward facing steps are commonly employed to establish recirculation zones for flame stability. Each method creates a low velocity zone of sufficient residence time and turbulence levels such that the combustion process becomes self-sustaining.

Traditional combustion systems depend on swirl stabilization, the TVC, instead, employs cavities to stabilize the flame. The availability of the literature on cavity flows contributes to its development [1,2,3,4]. Much of this effort examines the flow field dynamics established by the cavities, as demonstrated in aircraft wheel wells, bomb bay doors and other external cavity structures. Cavities have also been studied as a means of cooling and reducing drag on projectiles and for scramjets and waste incineration [5]. Very little work, however, exists on studying cavity flameholders for subsonic flow [4]. and none at all for lean premixed operation for potential use in a land based gas turbine engine.

The actual stabilization mechanism facilitated by the TVC is relatively simple. A conventional bluff or fore body is located upstream of a smaller bluff body - commonly referred to as an aft body - at a prescribed distance commensurate with cold flow stabilization studies [1,2,4]. The flow issuing from around the first bluff body separates as normal, but instead of developing shear layer instabilities which in most circumstances is the prime mechanism for initiating blowout, the alternating array of vortices are conveniently trapped or locked between the two bodies. The very stable yet more energetic primary/core flame zone is now very resistant to external flow field perturbations, yielding extended lean and rich blowout limits relative to its simple bluff body counterpart.

Due to its configuration, the system has greater flame holding surface area and hence will facilitate a more compact primary/core flame zone; which is essential in promoting high combustion efficiency and reduced emissions. Incorporation of transverse struts [4], which enhance the mixing/interaction of hot combustion products with the cooler premixed fuel and air, further reinforces the merits of the TVC as an excellent candidate for a lean-premixed combustion system. Furthermore, since part of combustion occurs within the recirculation zone, a typically flameless (Mild or Flox) regime can be achieved.

The objectives of this work are the evaluation of the performances and the stability regimes of a double cavity TVC by means of numerical simulations. The simulations are performed with a commercial code since this combustor is used in the industrial field.

Another aim of this research is to contribute to improve the knowledge and understanding of the physics involved in the TVC combustion and cover the lack of numerical [6,7] results regarding the use of this kind of combustor.

2 THE DOUBLE CAVITY TRAPPED VORTEX COMBUSTOR

Trapped Vortex Combustion technology is a positive promise in a wide range of industrial application. Conceived in the early 1990s for aeronautical propulsion, the research organizations initiated the design for gas turbine applications for energy production in the early 2000s.

The main characteristics of this kind of combustor are: compact dimensions, improved efficiency, lower emissions, greater flame stability, added fuel flexibility, increased durability, and reduced capital costs.

In the TVC the flame is stabilized through the use of cavities. The first design made use of two cavities, later developments employed one cavity. In both case a common feature, even with some kind of non-TVC concepts, is the creation of a toroidal flow reversal that recirculates and entrains a portion of the hot combustion products to mix with the incoming air and fuel to stabilize the flame.

A critical design feature involves the study of optimized geometric dimensions of the combustion chamber and of incoming air and fuel mass flow rates to trap stable flame toroidal vortices in the cavities. These flame zones are resistant to external flow field perturbations and therefore are less sensitive to instabilities and process upsets.

The combustion efficiency achieved and the gaseous emissions generated both depend strongly on the cavity loading and equivalence ratio. Unfortunately, depending upon the mainstream air entrained into the cavities, the actual values of these quantities can not be estimated directly from the metered fuel and air masses supplied to the combustor [6].

The TVC object of the numerical analysis has a double cavity and is fed with hydrogen. The facility, where the TVC is installed, is the MICOS (Multipurpose Installation for Combustion Studies) at the ENEA Casaccia, Rome.

2.1 ENEA TVC GEOMETRY

A TVC combustor has been designed and built at ENEA in 2008 under the framework of a research program focused on mild combustion. The ENEA TVC combustor (figure 1) consists of two majors portions: a centerbody assembly and, a housing assembly.

The centerbody assembly is formed from a long central shaft of stainless steel that is made up of an inner fuel tube surrounded by a concentric air passage with outer diameter, d_i, of *14 mm*, and which passes with a sliding fit through a solid disk of *100 mm* diameter, d_f, that forms a forebody. On the down stream half of the shaft is permanently mounted a short, hollow drum of *71.8 mm* diameter, d_a, that forms an afterbody. The drum contains two inner compartments that form respectively, primary air and fuel manifolds. These manifolds are supplied through the supporting double-tube shaft . The adjustable spacing *H*, between the forebody, the afterbody and the shaft forms the first annular cavity within which a vortex may be trapped. On the down stream end of the shaft is mounted another disk, the second afterbody. The second vortex is trapped in the cavity formed by the first and second afterbody.

Figure 1: ENEA TVC. The disk with holes is for CH_4.

Fuel is discharged upstream into the vortex cavity from the upstream face of the drum via a ring of 8 non-circular jets (figure 2) each of *63.24 mm*^{2} area; tubes from the fuel manifold pass through the air manifold to feed these jets. Air from the air manifold is discharged upstream into the vortex cavity from the upstream a face of the drum via two concentric rings of circular jets each of *3.25 mm* diameter. There are 8 air jets in the inner ring and 16 air jets in the outer. The ring of fuel jets is concentric with and between, the rings of air jets. The fuel jets are circumferentially oriented to place a fuel jet midway between adjacent pairs of inner and outer air jets.

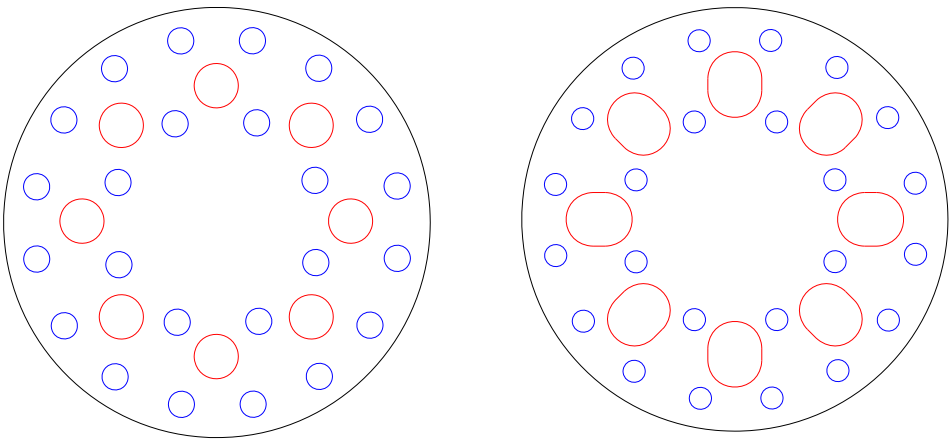

a) Plate for the CH_4: 8 holes for the fuel (red), 24 holes for the air (blue).

b) Plate for the H_2: 8 holes for the fuel (red), 24 holes for the air (blue).

Figure 2: ENEA TVC. The disk with holes is for CH_4.

The forebody is supported concentric in a duct of *113 mm* internal diameter, d_e, that supplies main/secondary air to the combustor from an air conditioning unit. The combustor main body is a length of *113 mm* internal diameter Quartz tubing. The length of the combustor is *475 mm*.

The wake region behind the afterbody provide a low speed region to consume the excess fuel, however, the vortex shedding can also cause local quenching. This can lead to reduced combustion efficiency. Adding a second afterbody results in a significant reduction in drag [8]. Basically, a second properly sized cavity results in another trapped-vortex between the first and second afterbody. The location of the second trapped-vortex would normally be the unsteady wake region of the afterbody, when only one afterbody is used. The second trapped-vortex reduces the drag because it reduces the unsteady wake motion. In a combusting flow, the second vortex should also reduce local quenching of the flame by reducing the flame-vortex quenching interactions. This was the idea leading to the two-cavity TVC.

The space between the first afterbody and the second afterbody is adjustable. The second afterbody has a *54 mm* diameter.

The complete centerbody assembly is cooled by the flows of air and fuel internally through it. The combustor main wall is protected from direct exposure to flame temperatures by the cool annular jet of main air that is in contact with it. No downstream external cooling of the main wall was provided. The forebody has no direct cooling, other than that provided by the annular flow of main air passing its outer edge.

3 NUMERICAL COMBUSTION MODELIZATION

A steady and unsteady, three dimensional, turbulent CFD simulation of the conservation equations for multicomponent reacting system has been performed considering also the energy equation to account for the temperature effects. The turbulence model adopted is a realizable k-ε which is implemented into the used CFD code. The turbulent reacting flame has been modelled using a finite rate approach taking into account detailed Arrhenius chemical kinetics.

The numerical scheme has been implemented using a parallel approach that can be opted in the commercial code presently used. The spatial discretization is performed using the finite volume approach and a second order accuracy is accomplished.

The study has been performed on a cluster for each test case allowing the management of a mesh with size optimized in terms of solution accuracy and reasonable calculation time. More details about the mesh size, the discretization properties and the combustion model are given in the following sections.

3.1 Computational domain and mesh properties

The geometry used for the calculation is that described in sec.2.1. Only a quarter of it is drawn. The size of the first cavity formed between the forebody and the disk is varied by moving the disk away from the forebody. In this way five geometries are obtainted. The cavity lengths of the five geometries are: 60, 65, 70, 75 and 80 mm. The computational domain is divided in many sub-domains to allow a better definition and a more flexible construction of the mesh. The length of the volume corresponds to the length of the TVC combustion chamber.

The grid generated from this geometry is hybrid (figure 3a). The zone, near the jet inlets on the first afterbody, is meshed with tetrahedral cells due to the particular shape of the holes (figure 3b). The remaining part of the domain is meshed with hexahedral cells (figure 3c).

The grid has been examined with a tool of the program obtaining good values for the equiangle skew (94 % of the elements lie between 0 and 0.4), the aspect ratio (96 % of the elements lie between 0 and 30) and the EquiSize skew (95 % of the elements lie between 0 and 0.4).

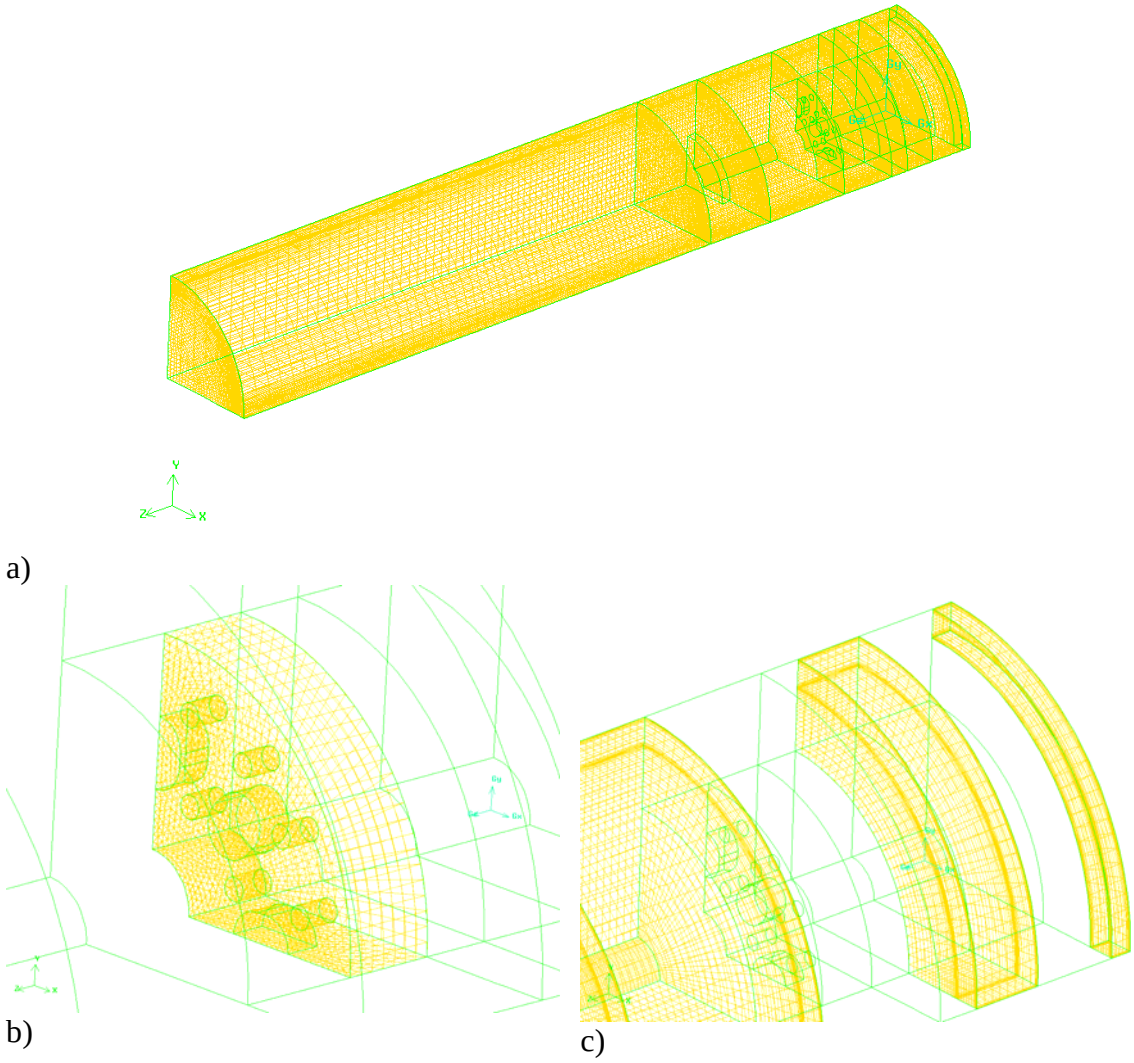

Figure 3: TVC discretization of the computational domain: a) whole domain b) Tetrahedral grid near the jet inlets c) hexahedral grid for some sub-domains.

3.2 Numerical model

This section examines the numerical model, showing some steps in the setup and solution procedure used for the TVC combustion computations.

The solver adopted is a pressure based solver with an implicit formulation.

The turbulent model is the realizable k-e because it more accurately predicts the spreading rate of both planar and round jets. It is also likely to provide superior performance for flows involving rotation, boundary layers under strong adverse pressure gradients, separation and recirculation.

In order to include radiation effects in the heat transfer simulations a radiation model is chosen. The more appropriate is the Discrete Ordinates (DO) model. The DO model spans the entire range of optical thicknesses, and allow to solve problems ranging from surface to surface radiation to participating radiation in combustion problems. The DO radiation model solves the radiative transfer equation (RTE) for a finite number of discrete solid angles, each associated with a vector direction fixed in the global Cartesian system. The finesses of the angular discretization is controlled by the user.

Computational cost is moderate for typical angular discretization, and memory requirements are modest but solving problem with fine angular discretization may be CPU-intensive. In the simulations the angular discretization has been incremented from the default values verifying that the new values did not become too much expensive for the CPU and memory resources.

Finally the achievement of a right compromise between the computational effort and the results accuracy leads to the choice of 3 angular divisions and a 2 x 2 pixelization.

The DO model also allows the solution of radiation at semi-transparent walls and opaque walls. In this way the right amount of absorbed, emitted and reflected energy from the wall surface can be taken into account.

The TVC forebody, first afterbody and second afterbody walls are considered as opaque walls made in steel while the TVC combustion chamber, made in quartz, is considered as semi-transparent.

All the physical and thermal properties of the steel and quartz are properly set in the code (see next table).

	Steel	Quartz
Density [kg/m^3]	8030	2203
Specific heat [J/kg-K]	502	703
Thermal conductivity [W/m-K]	16.27	1.33
Refractive index	-	1.46
Emissivity	0.8	0.93

Table 1: Steel and quartz thermal and physical properties.

The combustion process in the TVC is solved using a finite rate reaction model based on the Arrhenius equation: the Eddy Dissipation Concept (EDC). It is an extension of the eddy dissipation model to include detailed chemical mechanism in turbulent flows. The detailed mechanism is reported in table 2.

The gas mixture is composed by 13 species: H H_2 H_2O H_2O_2 HO_2 HNO N N_2 N_2O NO O O_2 OH.

For each species in the gas mixture the properties in tables 3 and 4 are set.

The thermochemical data needed to compute the specific heat coefficient and the transport data containing the Lennard Jones coefficient are taken from GRI-Mech 3.0.

Due to the presence of gas phase species as combustion products the absorption in the gas is significant. The WSGGM option is used to take into account a variable composition dependent absorption coefficient.

WSGGM stands for Weighted Sum of Gray Gases Model. It is a reasonable compromise between the oversimplified gray gas model and a complete model which takes into account particular absorption bands.

No.	Reaction	A	n	E_a
R.1	$H+O_2=OH+O$	2.00E+14	0	70.3
R.2	$H_2+O=OH+H$	1.80E+10	1	36.93
R.3	$H_2O+O=OH+OH$	5.90E+09	1.3	71.25
R.4	$H_2+OH=H_2O+H$	1.17E+09	1.3	15.17
R.5	$H+O_2+M^a=HO_2+M^a$	2.30E+18	-0.8	0
R.6	$H+HO_2=OH+OH$	1.50E+14	0	4.2
R.7	$H+HO_2=H_2+O_2$	2.50E+13	0	2.93
R.8	$OH+HO_2=H_2O+O_2$	2.00E+13	0	4.18
R.9	$H+H+M^a=H2+M^a$	1.80E+18	-1	0
R.10	$H+OH+M^a=H_2O+M^a$	2.20E+22	-2	0
R.11	$HO_2+HO_2=H_2O_2+O_2$	2.00E+12	0	0
R.12	$H_2O_2+M=OH+OH+M$	1.30E+17	0	190.38
R.13	$H_2O_2+OH=H_2O+HO_2$	1.00E+13	0	7.53
R.14	$O+HO_2=OH+O_2$	2.00E+13	0	0
R.15	$H+HO_2=O+H_2O$	5.00E+12	0	5.9
R.16	$H+O+M=OH+M$	6.20E+16	-0.6	0
R.17	$O+O+M=O_2+M$	6.17E+15	-0.5	0
R.18	$H_2O_2+H=H_2O+OH$	1.00E+13	0	15.02
R.19	$H_2O_2+H=HO_2+H_2$	4.79E+13	0	33.26
R.20	$O+OH+M=HO_2+M$	1.00E+16	0	0
R.21	$H_2+O_2=OH+OH$	1.70E+13	0	200
R.22	$O+N_2=N+NO$	1.82E+14	0	319.02
R.23	$O+NO=N+O_2$	3.80E+09	1	173.11
R.24	$H+NO=N+OH$	2.63E+14	0	210.94
R.25	$NO+M=N+O+M$	3.98E+20	-1.5	627.65
R.26	$N_2+M=N+N+M$	3.72E+21	-1.6	941.19
R.27	$N_2O+O=NO+NO$	6.92E+13	0	111.41
R.28	$N_2O+O=N_2+O_2$	1.00E+14	0	117.23
R.29	$N_2O+N=N_2+NO$	1.00E+13	0	83.14
R.30	$N+HO_2=NO+OH$	1.00E+13	0	8.31
R.31	$N_2O+H=N_2+OH$	7.60E+13	0	63.19
R.32	$HNO+O=NO+OH$	5.01E+11	0.5	8.31
R.33	$HNO+OH=NO+H_2O$	1.26E+12	0.5	8.31
R.34	$NO+HO_2=HNO+O_2$	2.00E+11	0	8.31
R.35	$HNO+HO_2=NO+H_2O_2$	3.16E+11	0.5	8.31
R.36	$HNO+H=NO+H_2$	1.26E+13	0	16.63
R.37	$HNO+M=H+NO+M$	1.78E+16	0	203.7

[a] H_2=1.0 H_2O=6.5 O_2=0.4 N_2=0.4.

Units are cm^3, mol, s, kJ and K

Table 2: Hydrogen chemical mechanism.

4 RESULTS

The present chapter reports the fundamental results of this research: the study of the performances of a double cavity trapped vortex combustor feed with hydrogen.

The main parameters varied for the simulations are described in the following paragraph. The simulations are made with the aim of understanding the behaviour of the combustor in different working conditions, to verify transient effects in the cavities and to describe the peculiar flow structures of this kind of combustor. Therefore the analysis presented is focused on describing the essential features of the TVC with particular regard on the temperature, the emissions, the velocity flow fields and the spectra, the last obtained analysing unsteady data from some probes put in the computational domain.

4.1 Test Matrix

The main parameters influencing the working conditions and varied during the simulations are:

- Power: three main powers 21, 42, 84 kW needed to make available data for the comparison with another power plant in ENEA Casaccia;
- Given three fixed secondary air velocities the power has been reduced starting from 84 kW to some kW;
- Distance between the forebody and the afterbody: 60, 65, 70, 75 and 80 mm;
- Equivalence ratio Φ (primary and secondary); the quantity changed are:
    - Fuel mass flow rate;
    - Primary air mass flow rate;
    - Secondary air mass flow rate;
- Secondary air composition:
    - Air with moisture;
    - Gas from a combustor;
    - Without primary air;
- Time dependence: steady and unsteady.

The complete list of the steady test cases studied is reported in the appendix.

The primary air and fuel jets control the local equivalence ratio, mixing, residence time, and stability in the primary zone. The maximum secondary (overall) equivalence ratio, calculated adding the secondary air, is about 0.2 which is below the LBO limit of typical swirl or bluff-body stabilized flames.. The actual equivalence ratio in the primary zone may be less than that calculated analytically due to the entrainment of annular air. However, the amount of entrainment changes with primary air and fuel flows and has not been evaluated.

4.2 Flow field and flame

The flow field in a small or large cavities is quite complex as a result of the formation of several vortices. Because of the presence of the cavities, the secondary air is expanded toward the centerbody, which, in turn, results in flow separations on the outer wall. The CFD solutions do provide valuable qualitative information to more fully understand the vortex structures in the cavities and the flow separations, but the present simulations predict only the large-scale vortical structures in the cavity, small scales important for mixing on a local level are not resolved.

Figure 4 and 5 show the trapped vortices behind the TVC disks. As can be seen in the figures, several distinct vortices are predicted in the TVC cavities. The velocity field shows a strong recirculating flow that is expected for toroidal vortices.

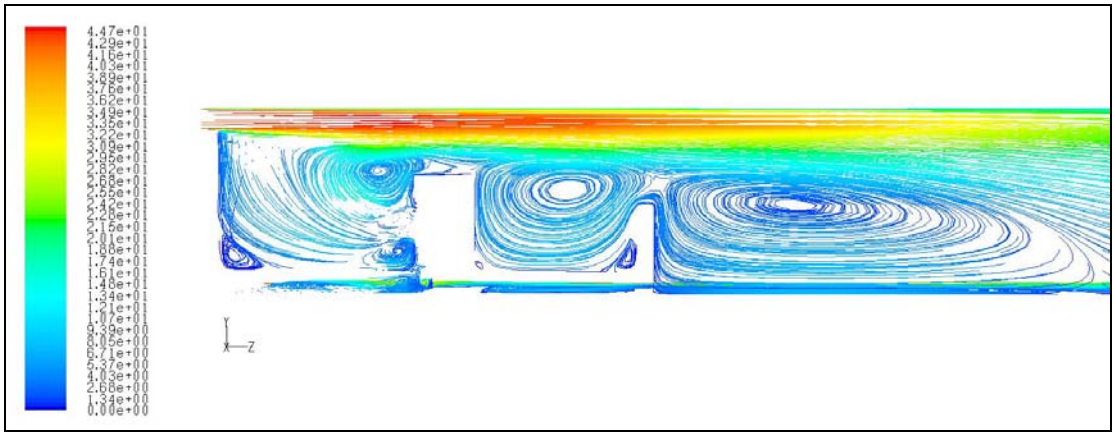

Figure 4: TVC Velocity Pathlines. Test case: P=21 kW, disk distance 60 mm, Y_{h2o}=0, ϕ_{prim}=1, $\phi_{overall}$=0.053.

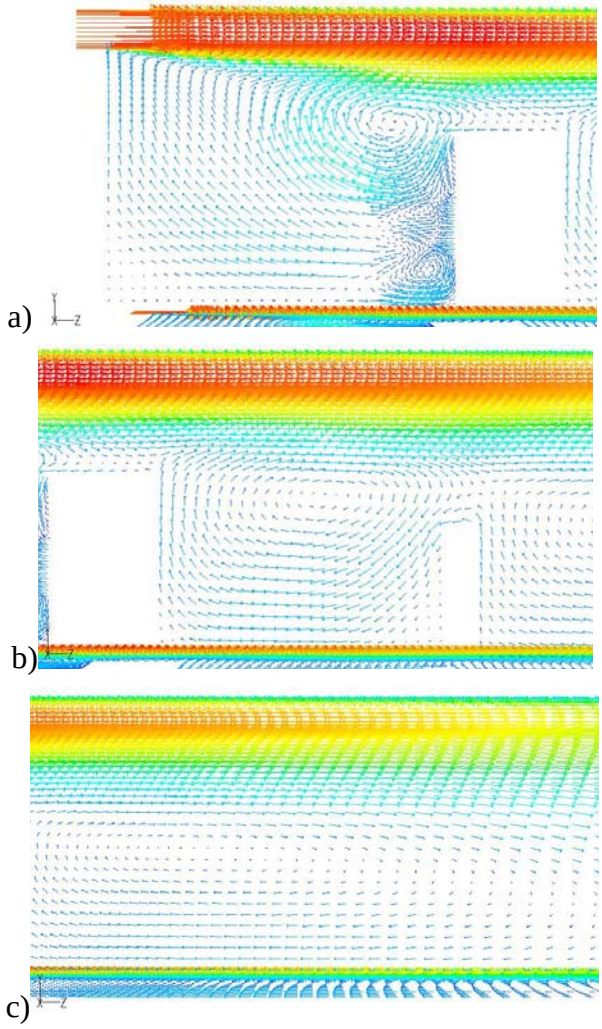

Figure 5: Velocity vector plots of the flow. a) First cavity b) Second cavity c) downstream the last disk. Test case: P=21 kW, disk distance 60 mm, Y_{h2o}=0, ϕ_{prim}=1, $\phi_{overall}$=0.053.

The main vortex in the first cavity rotates with the secondary air flow direction figure 5a due to the placement of the fuel and air injection points. But depending on the location and flow rates of the injection points, cavity vortices rotating in opposition or with the secondary air flow direction can be generated [3]. The vortices in the second cavity figure 5b and behind the second afterbody figure 5c also rotate with the annular air flow.

In general the center fuel jet is mixed with the neighbouring air jets and burns as a singular flame. The figure 4 and 5a suggests that flow in the first cavity has a large vortex generated by the secondary air flow and a secondary vortex that have developed primarily from the interaction of fuel and air jets injected in the cavity. There is also a third vortex in the left corner due to the motion of the mixture flow. The vortex trapped in the cavity provides a sufficiently stable ignition source through re-ingestion of hot products and radicals back into the recirculation zone, as indicated by the velocity field.

The general structure of the larger vortex in the first cavity appeared to be the same for a wide range of fuel and air flow conditions. Decreasing the secondary air mass flow rate the large vortex reduces its dimensions (figure 6) reducing the amount of re-ingested hot products.

Instead, with the secondary air mass flow rate fixed, decreasing the primary air mass flow rate the vortex progressively grows occupying the entire cavity (figure 7). Best results in terms of mixing are obtained when the vortex occupies the entire cavity.

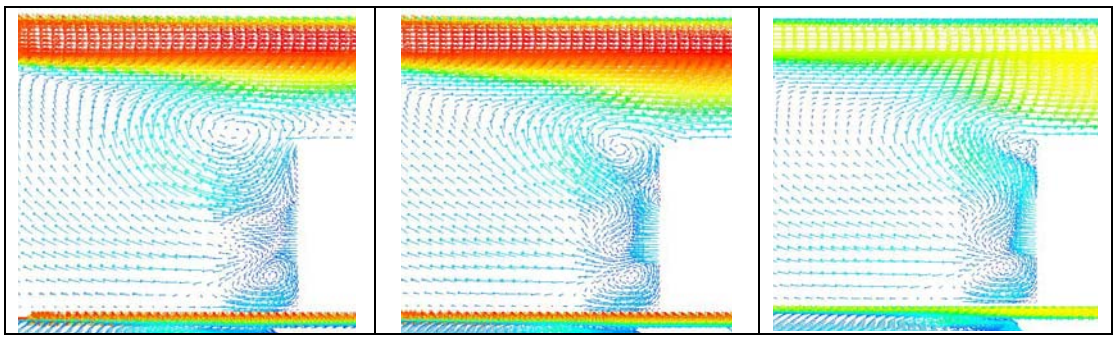

Figure 6: Effect of the secondary air mass flow rate reduction on the trapped vortex dimensions. Primary air mass flow rate and all other parameters fixed.

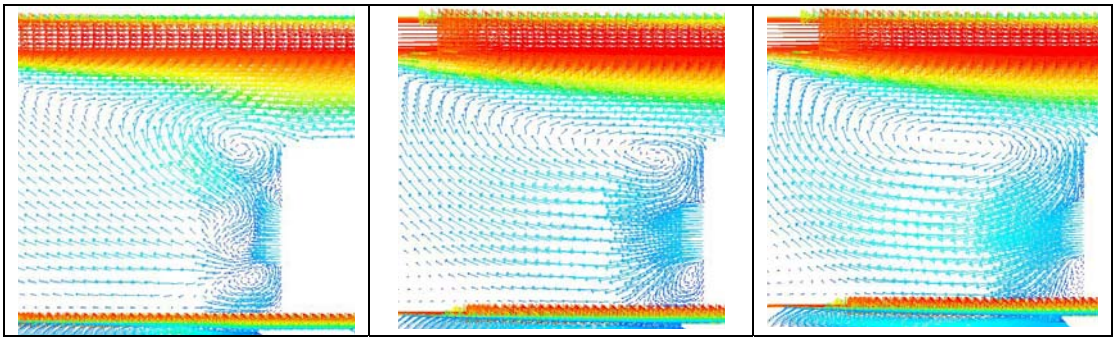

Figure 7: Effect of the primary air mass flow rate reduction on the trapped vortex dimensions. Secondary air mass flow rate and all other parameters fixed.

For what concern the flame front, it depends on the various regimes established in the combustor.

Increasing the power (figure 8) or decreasing the primary or secondary air flow rate the flame bulges out radially toward the annular air, can reach the second cavity or pass

the second afterbody. In the last case the flame can have a length comparable with the TVC length (*47.5 cm*).

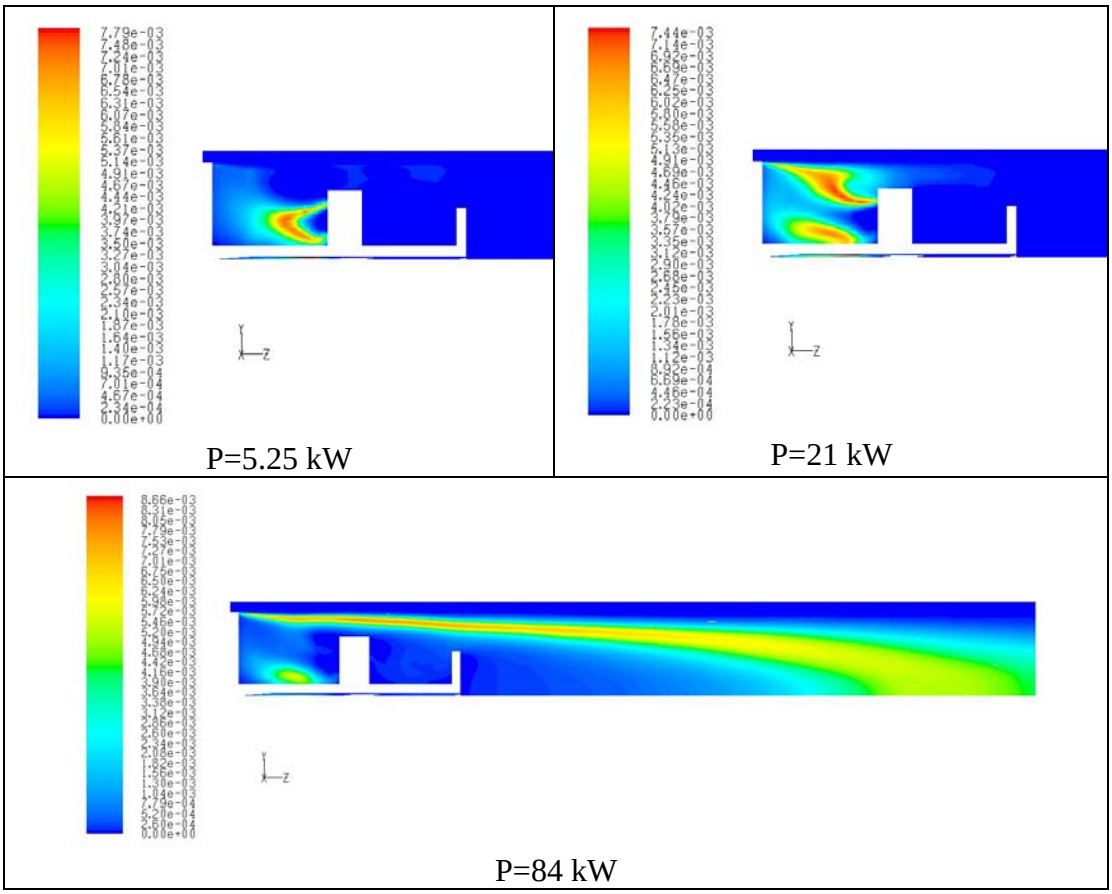

Figure 8: Mass fraction of OH. Effect of varying power on the flame structure. The primary and overall equivalence ratio are fixed to: ϕ_{prim}=1, $\phi_{overall}$=0.053. The disk distance is set to 60 mm.

4.3 Effect of moisture

The effect of moisture on the combustion characteristics of the TVC has been tested adding a fixed value of water mass fraction in the secondary air composition. The simulated cases include three powers: *21*, *42* and *84 kW*. For each power the distance of the disk is varied by *5 mm* from *60* to *80 mm*.

The maximum temperature and the mean exit temperature decreases adding moisture. The mean temperature variation is very low due to the low ratio of water injected with the secondary air. Adding more water the variation will be more significant.

The combustion efficiency in almost all cases is not on a direct correlation with the added water.

The addiction of the ambient humidity to the air decreases the NOx emission indices as shown in figure 9.

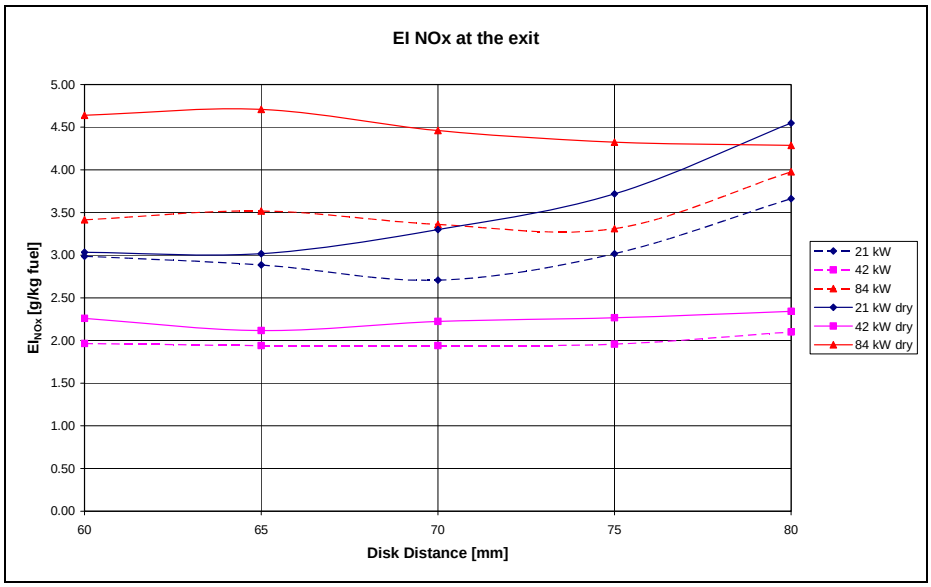

Figure 9: NOx emission indices as a function of the disk distance for dry and humid air.

4.4 Effect of the primary and secondary equivalence ratio

The quantity of fuel injected is fixed at a mass flow rate corresponding to a power of 21 kW and the annular / secondary air flow is fixed at three quantities corresponding to velocities of 11, 22 and 44 m/s. Emissions data are then collected for different primary air flow rates.

The results show that the TVC works in a wide range of primary equivalence ratio even for very low quantity of primary air. When the primary air flow is low the air needed to burn the fuel is entrained into the trapped vortex from the secondary flow.

The mean exit temperature (figure 10), the values of the combustion efficiency and the NOx emissions decrease as the secondary air increase. For the cases analysed, there is not a direct correlation with lower value of the primary equivalence ratio.

The values of UHC and NOx (figure 11) emission index are very similar to those reported in [1].

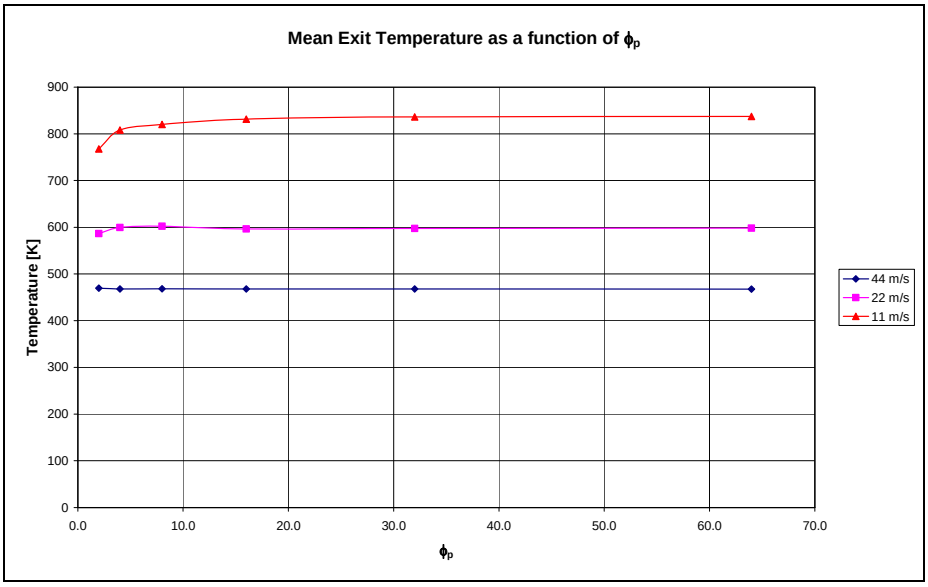

Figure 10: Mean exit temperature in the TVC as a function of the primary equivalence ratio for three secondary air flow velocities.

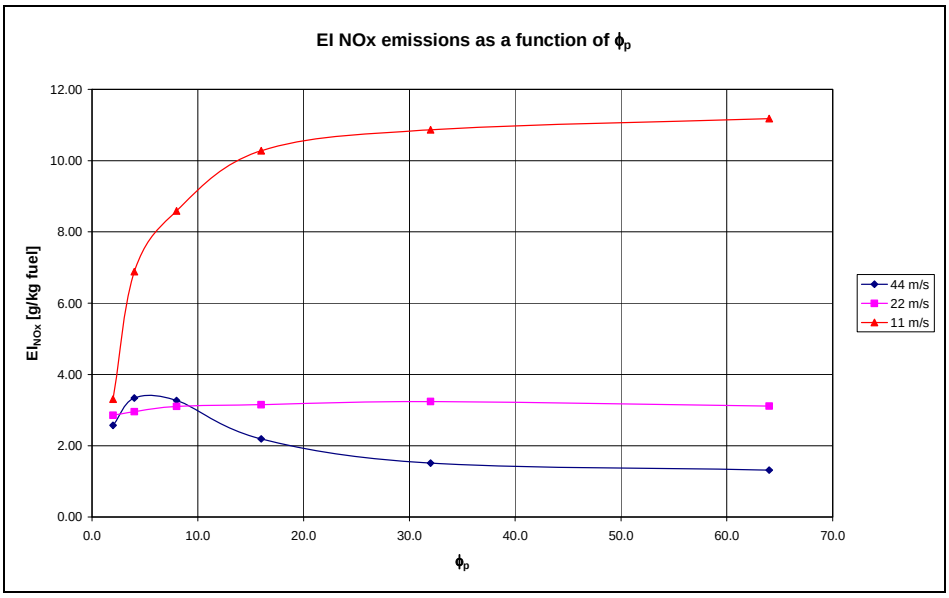

Figure 11: Impact of primary and annular air on the NOx emission index at fixed fuel flow.

4.5 Combustion instabilities

Several investigators [8] demonstrated that mounting two disk in tandem can reduce the drag resulting from the unsteady vortex motion behind the disks.

Flow oscillations, studied in works such as [5], were found to be established under certain geometric aspect ratio and resulted from impingement associated with shear layer and cavity corner.

In the TVC, in addition to the oscillatory phenomena for non reacting flow it must be considered instabilities due to the combustion process.

In Combustion, the instabilities are a result of the resonant interaction between two or more physical mechanisms. A driving process generates the perturbations of the flow; a feed back process couples the perturbation to the driving mechanism and produces the resonant interaction that may lead to oscillatory combustion. The heat release can amplify certain flow frequencies [9].

The flame stability in the TVC is directly related to the annular air and its interaction with the cavity. There are two possible interactions:

- The shear layer along the interface between the annular and cavity regions;
- The impingement region near the afterbody.

The first physical process increases with annular air velocity and can affect flame stability in the cavity. If the cavity is small, the disturbance in the shear layer is less likely to have impact on the cavity.

Increasing the cavity length, the possibility of disturbance from shear layer and flow impingement at the upstream face of the afterbody become higher. The last case results in high pressure fluctuations and high drag, and reduces the stability of the cavity combustion.

Two cases are reported to verify this phenomena. The power is set to 21 kW. In the first case the disk distance is fixed at 60 mm while in the second case at 70mm. For all cases the time step is fixed at 0.001 ms according to [7]. The mass flow rates are set to obtain the primary and overall equivalence ratios reported in table 5.

Test Case	Power [kW]	Disk Distance	Φ_{prim}	$\Phi_{overall}$
1	21	60	1	0.053
2	21	70	4	0.401

Table 5: Unsteady analysis test matrix.

Power spectral density of the velocity, the pressure and the temperature for the first case at one location inside the cavity have been calculated. In every spectrum there is a dominant frequency peak in the lower frequency range. The peak is placed at about 40 Hz corresponding to St= 0.06. According e.g. to [10] the low value of St is not compatible with the shear layer instability but it may be due to a flapping motion of the recirculation bubble.

The frequency of the flame oscillation corresponds to a time delay of *25 ms*. The oscillating phenomena is visualized through a time sequence of OH contour plots shown in figure 16. The time interval between two consecutive images is 2 ms. It can be noticed how initially the flame is attached to the forebody, then as time goes on the flame progressively detaches from the forebody, reaches a maximum distance (*t=12ms*) and after about *25 ms* it returns to the starting position. The instantaneous solutions of this flow revealed that the vortices in the cavity are not shedding but moving back and forth within the cavity.

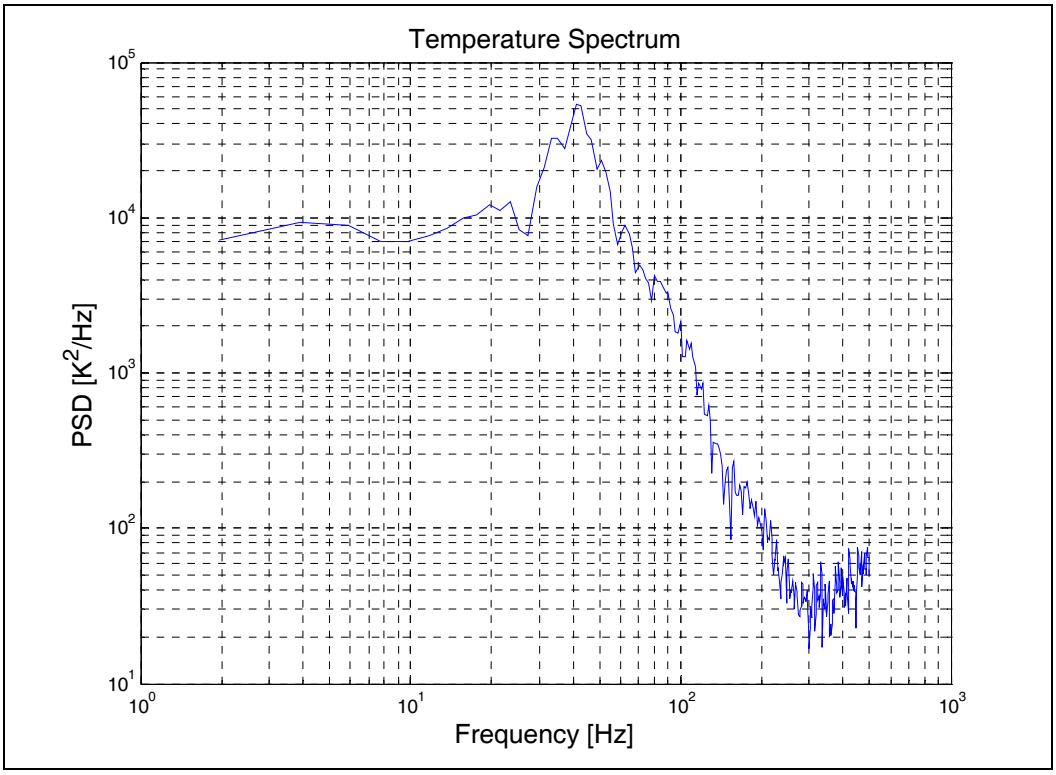

Figure 12: Temperature spectrum for the first case: *Φ=1, P=21 kW, H=60mm.*

As the primary air flow is reduced, keeping the same distance between disks, the fuel jet is pushed further toward the centreline of the burner, increasing the possibility of the flow impingement. The combination of the increased level of flow impingement and lack of fuel transport towards the edge of the forebody is believed to be the reason of a reduced flame stability. In the sequence after the impingement, the flame returns to the initial state. This oscillating regime led to the flame blowout. The results are not reported here.

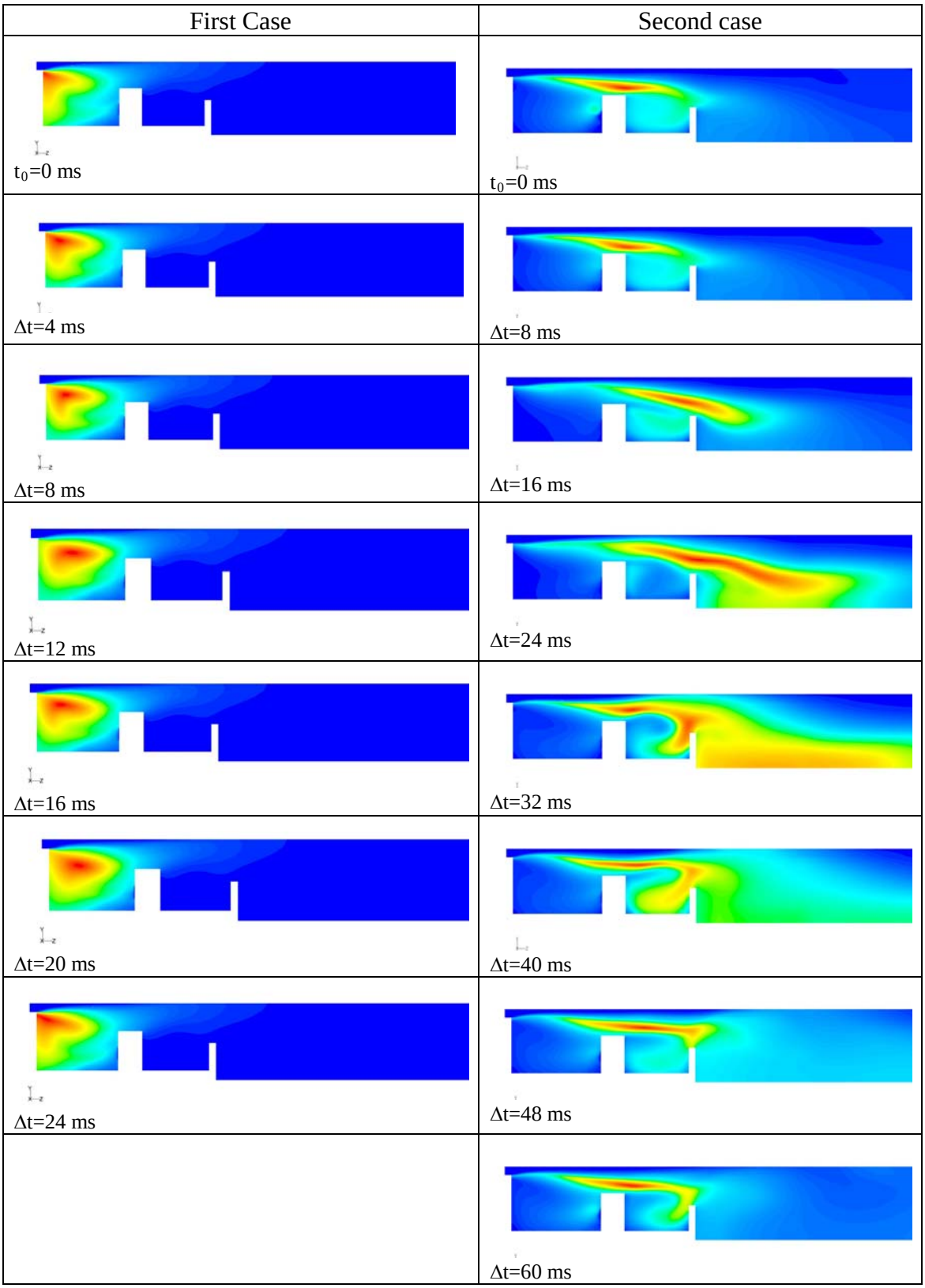

Figure 16: Time sequences contour plot of OH mass fractions for the first and third case visualizing the oscillating phenomena (at 40 Hz and 15 Hz respectively). The scale is comprised between 0 and 0.0032.

In the second case the fuel is not consumed in the primary vortex but is transported in the shear layer at the rim of the first afterbody obtaining a flame that bulges out the first cavity. The flame is anchored, not stable but it does not reach the blow out limit.

The oscillations take place in the two trapped vortex cavities and behind the bluff body represented by the second afterbody. The second vortex in the second cavity serves as a secondary mixing and combusting stage because some fraction of the reacting mixture burns out when mixed with the hot products that are transported out of the vortex. This is confirmed by the presence of OH radicals in the second cavity (see figure 16).

The flame and the hot products are then periodically convected downstream of the second cavity and entrained into the wake region behind the second afterbody (figure 16 $\Delta t=24ms$ to $\Delta t=40\ ms$) or carried on downstream toward the TVC exit.

Power spectral densities of the velocity, pressure and temperature for the third case at various location inside the cavity are calculated. Only the temperature spectra are presented (figure 13 to 15). In every spectrum there is not only a dominant frequency peak in the lower frequency range as in the first case but a series of peaks due to the oscillations of the vortices in the three cavities. However in every spectrum there is a peak at about 15 Hz (60 ms).

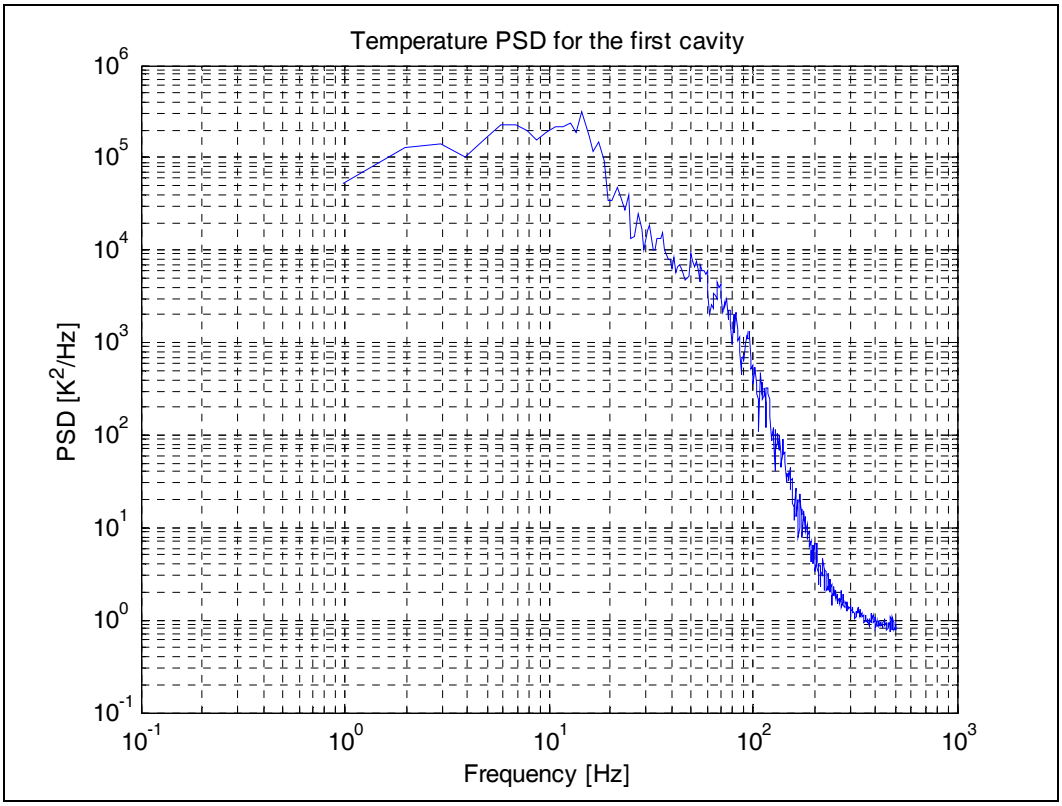

Figure 13: Temperature spectrum for the first case, first cavity: $\Phi_{prim}=4$, $P=21\ kW$, $H=70mm$.

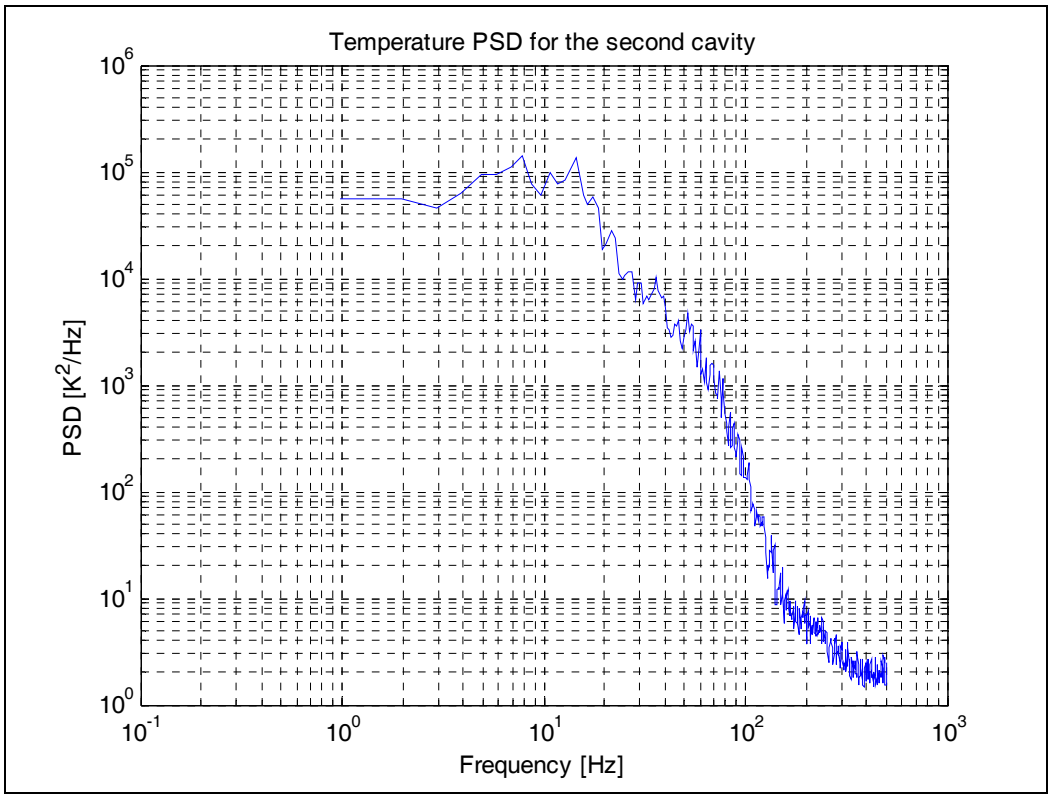

Figure 14: Temperature spectrum for the first case, second cavity: Φ_{prim}*=4, P=21 kW, H=70mm.*

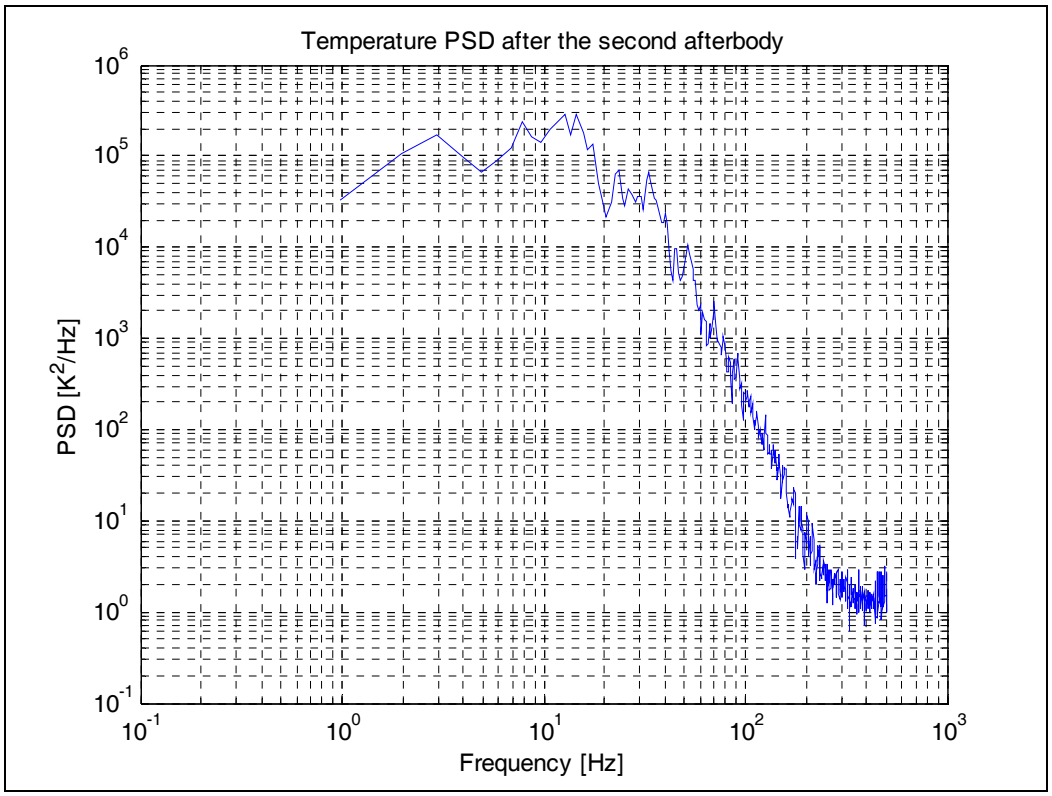

Figure 15: Temperature spectrum for the first case, after the second afterbody: Φ_{prim}*=4, P=21 kW, H=70mm.*

5 CONCLUSIONS

The performances and the stability of the ENEA TVC has been numerically investigated. The geometry is based on the one proposed by [1]. In this kind of combustor two cavities are sized to trap vortices when air flow passes through. Fuel and primary air are injected directly into the vortex from multiple jets in the down stream wall of the first cavity. The underlying idea of the TVC is that the flame, once established in the trapped vortex, should remain stable over a wide range of operating conditions. This idea is assessed in the present work and the main parameters - power, distance of the first cavity disks, primary and secondary equivalence ratios, humidity - are examined for several test cases.

The 3D-CFD simulations depict several distinct vortices in the TVC cavities. In the all analysed cases three main vortices develop: two in the first and second cavity and one behind the last disk, as an effect of the shear layer. In the first cavity arise both a secondary vortex, mainly because of the interaction between fuel and air jets injected in the cavity, and a third vortex, due to the motion of the mixture flow. Depending on the quantity of primary or secondary air mass flow rate, the dimension of the main vortex in the first cavity can change. This vortex is responsible of the air-fuel-hot product mixing. By reducing the dimensions, the amount of re-ingested hot products is low. Best results are obtained when the vortex spreads over the entire cavity.

For what concern the flame front, it depends on the various regimes established in the combustor. Depending on the power and on the primary and secondary air flow rate, the flame can be confined in the first cavity or bulged out radially toward the annular air, reaching the second cavity or passing the second afterbody. When the flame is confined in the first cavity, the primary zone may not be affected by entrainment of cold annular air. The higher temperatures at this condition result in good combustion efficiency, but higher NOx.

The effect of moisture on the combustion has been tested adding a fixed value of water mass fraction in the secondary air composition. Results do not show a direct correlation between combustion efficiency and added water, while lower NOx emission indices has been obtained by adding ambient humidity. For future development it could be useful to inject water directly into the combustion airstream, a technique commonly used in gas turbine combustion to enhance efficiency and decrease emissions at lower costs.

The TVC works in a wide range of primary and secondary equivalence ratios, reaching overall values below common limits for gas turbine combustors. Results obtained increasing the secondary air flow show the decrease of the mean exit temperature, of the combustion efficiency value and of the NOx emissions. It is noticed that in all the analysed cases the value of the efficiency is always higher than 97%. This means that only a maximum of 3% of the fuel is not consumed.

Another TVC feature studied is the combustion instability. Two kind of instabilities have been detected, both directly related to the annular air and its interaction with the cavity. The first is due to the interaction of the shear layer along the interface between the annular and cavity regions, while the impingement region near the afterbody causes the second one. Referring to the first instability, the instantaneous solutions have revealed that the vortices in the cavity are not shedding, but moving back and forth within the cavity. The spectra show a peak corresponding to St=0.06, a low value due to a flapping motion of the recirculation bubble.

Increasing the distance between the disk and maintaining a low primary flow rate (primary equivalence ratio of about 4), the flame resulted anchored but not stable. The oscillations take place in the trapped vortex cavities and behind the second afterbody. In

every spectrum obtained from some probes, opportunely placed in the domain, there is not a dominant frequency peak in the lower frequency range, but a series of peaks, mostly because the vortices oscillations due to the combustion take place in the three cavities.

In conclusion, the ENEA TVC offers a wide range of operating conditions with reasonable combustion efficiency and low emissions in a simple and compact combustor. However, further work is required. For future study, Large Eddy Simulation (LES) will be utilized in the numerical code to predict smaller scale structures and quantities fluctuations. More working conditions should be examined to better understand the dynamic behaviour of the TVC and to evaluate methods for maintaining good performance characteristics while substantially reducing NOx.

REFERENCES

[1] K.-Y. Hsu, L.P. Goss, D.D. Trump, and W.M. Roquemore, Performance of a Trapped Vortex Combustor, In the proceedings of the 33rd *Aerospace Science Meeting and Exhibit*, January 9-12, Reno, NV, AIAA Paper 95-0810 (1995)

[2] G.J. Sturgess and K.-Y. Hsu, Entrainment of mainstream flow in a trapped vortex combustor, In the proceedings of the 35th *Aerospace Science Meeting and Exhibit*, January 6-9, Reno, NV, AIAA Paper 97-0261 (1997)

[3] D.L. Straub, T.G. Sidwell, D.J. Maloney, K.H. Casleton, G.A. Richards, W.A. Rogers and G.M. Golden, Simulations of a Rich Quench Lean (RQL) Trapped Vortex Combustor, presented at the *American Flame Research Committee (AFRC) International Symposium*, Newport Beach, CA (2000)

[4] W.M. Roquemore, D. Shouse, D. Burrus, A. Johnson, C. Cooper, B. Duncan, K.-Y. Hsu, V.R. Katta, G.J. Sturgess and I. Vihinen, Trapped Vortex Combustor Concept for Gas Turbine Engines, in the proceedings of the 39th *Aerospace Sciences Meeting and Exhibit*, January 8-11, Reno, NV AIAA Paper 2001-0483 (2001)

[5] M. Gharib and A. Roshko, The Effect of Flow Oscillations on Cavity Drag. *Journal of Fluid Mechanics* **177**, pp. 501-530 (1987)

[6] C. Bruno and M. Losurdo, The Trapped Vortex Combustor: and advanced combustion technology for aerospace and gas turbine applications, *Advanced Combustion and Aerothermal Technologies*, pp. 365-384 (2007)

[7] V.R. Katta and W.M. Roquemore, Numerical Studies on Trapped-Vortex Combustor, In the proceedings of the 32nd *AIAA/ASME/SAE/ASEE Joint Propulsion Conference*, July 1-3, Lake Buena Vista, FL, AIAA Paper 96-2660 (1996)

[8] W.A. Mair, The effect of a Rear-Mounted Disc on the Drag of a Blunt Based body of revolution, *The Aeronautical quarterly*, **16**, 350-360 (1965);

[9] K.-Y. Hsu, C.D. Carter, V.R. Katta, and W.M. Roquemore, Characteristics of combustion instability associated with trapped-vortex burner, in the proceedings of the 37rd *Aerospace Science Meeting and Exhibit*, January 11-14, Reno, NV, AIAA Paper 99-0488 (1999)

[10] M. Kiya and K. Sasaki, Structure of a turbulent separation bubble, *J. Fluid Mech.* **137**, pp. 83-113 (1983)